

Planetary Orbital Equations in Externally-Perturbed Systems: Position and Velocity-Dependent Forces

Dimitri Veras · N. Wyn Evans

Received: 02 July 2012 / Revised: 27 September 2012 / Accepted: 24 October 2012

Abstract The increasing number and variety of extrasolar planets illustrates the importance of characterizing planetary perturbations. Planetary orbits are typically described by physically intuitive orbital elements. Here, we explicitly express the equations of motion of the *unaveraged* perturbed two-body problem in terms of planetary orbital elements by using a generalized form of Gauss' equations. We consider a varied set of position and velocity-dependent perturbations, and also derive relevant specific cases of the equations: when they are averaged over fast variables (the “adiabatic” approximation), and in the prograde and retrograde planar cases. In each instance, we delineate the properties of the equations. As brief demonstrations of potential applications, we consider the effect of Galactic tides. We measure the effect on the widest-known exoplanet orbit, Sedna-like objects, and distant scattered disk objects, particularly with regard to where the adiabatic approximation breaks down. The *Mathematica* code which can help derive the equations of motion for a user-defined perturbation is freely available upon request.

Keywords Perturbation Methods; Computer Methods; Planetary Systems; Comets and Meteors

1 Introduction

The discovery of extrasolar planets challenged our understanding of the formation and subsequent evolution of planetary systems. The variety of dynamical

Dimitri Veras
Institute of Astronomy, University of Cambridge, Madingley Road, Cambridge CB3 0HA
Tel.: +44 (0)1223 337548
Fax: +44 (0)1223 337523
E-mail: veras@ast.cam.ac.uk

N. Wyn Evans
Institute of Astronomy, University of Cambridge, Madingley Road, Cambridge CB3 0HA
E-mail: nwe@ast.cam.ac.uk

architectures demonstrated by pulsar planets (e.g. Wolszczan & Frail, 1992), Hot Jupiters (e.g. Mayor & Queloz, 1995), wide-orbit planets (e.g. Kuzuhara et al., 2011; Luhman et al., 2011), free-floating planets (e.g. Lucas & Roche, 2000; Zapatero Osorio et al., 2000; Sumi et al., 2011), highly inclined and retrograde planets (e.g. Anderson et al., 2010; Triaud et al., 2010; Winn et al., 2010; Kaib et al., 2011), closely-packed planets (e.g. Lissauer et al., 2011), circumbinary planets (e.g. Sigurdsson et al., 2003; Doyle et al., 2011) and the Solar System defy a single, simple explanation for their formation.

After formation, these systems are subjected to internal forces, from planets and smaller bodies, and external forces, such as the singular or repeated local close encounters with individual passing stars, the Galactic tide, tidal tails, molecular clouds, globular clusters or even dark matter substructures. Further, a star’s passage into and out of spiral arms, and the deformation of the Galactic tide due to close encounters or collisions with other galaxies can affect orbiting planets¹. One known exoplanet is thought to be of extragalactic origin, perhaps originating from a disrupted satellite galaxy (Setiawan et al., 2010). The vast population of free-floating planets – nearly two per main sequence star (Sumi et al., 2011) – which cannot be explained by planet-planet scattering alone (Veras & Raymond, 2012), perhaps demonstrates that external disruption of planetary systems is an endemic feature of the Galactic disk.

Some of these external forces may be modeled as perturbations on a two-body star-planet system. Although the two-body problem is solvable analytically, the perturbed two-body problem is generally not so. Nevertheless, expressing these equations of motion entirely in terms of planetary orbital elements garners intuition for how planets are affected by external perturbations and helps one obtain analytical solutions in limiting cases. Here, we present a method for performing this conversion for arbitrary perturbations.

Suppose the equations of motion for a single planet orbiting a single star are subject to extra accelerations Υ . Then the equations of motion can be expressed as:

$$\frac{d^2x}{dt^2} = -\frac{G(m_\star + m_p)x}{(x^2 + y^2 + z^2)^{3/2}} + \Upsilon_{xx}x + \Upsilon_{xy}y + \Upsilon_{xu}\frac{dx}{dt} + \Upsilon_{xv}\frac{dy}{dt} \quad (1)$$

$$\frac{d^2y}{dt^2} = -\frac{G(m_\star + m_p)y}{(x^2 + y^2 + z^2)^{3/2}} + \Upsilon_{yx}x + \Upsilon_{yy}y + \Upsilon_{yu}\frac{dx}{dt} + \Upsilon_{yv}\frac{dy}{dt} \quad (2)$$

$$\frac{d^2z}{dt^2} = -\frac{G(m_\star + m_p)z}{(x^2 + y^2 + z^2)^{3/2}} + \Upsilon_{zz}z + \Upsilon_{zw}\frac{dz}{dt} \quad (3)$$

where m_\star and m_p represent the masses of the star and planet, respectively. In the context of a single planet orbiting the Galactic center, we may take (x, y, z) to be a non-rotating rectangular coordinate system centered on the

¹ The Milky Way and Andromeda will collide in $\sim 2\text{--}5$ Gyr, before many Galactic stars, including the Sun, turn off of the main-sequence (Cox & Loeb, 2008; van der Marel et al., 2012).

star, as in Heisler & Tremaine (1986). The primary goal of this paper is to express Eqs. (1)-(3) analytically in terms of the time evolution of planetary orbital elements. The secondary goal is to present the method by which one can repeat the procedure for other perturbational forms not included in Eqs. (1)-(3).

In Section 2, we provide background for the perturbed two-body problem and present the algorithm used to derive the equations. We then present the general equations in Section 3. Sections 4 and 5 specialise to the adiabatic and planar adiabatic cases, for which substantial simplifications are possible. We provide applications to perturbations derived from the Galactic tides in Section 6 and summarize our results in Section 7.

2 Background and Derivation Algorithm

In order to describe fully the position and velocity of a planet, 6 orbital elements must be employed. Four often-used elements are the semimajor axis, a , eccentricity, e , inclination, i , and the longitude of ascending node, Ω . A fifth orbital element usually includes the longitude of pericenter, ϖ , or the argument of pericenter, ω . The difference is important here, and they are related through $\omega + \Omega = \varpi$. All five of these elements fully describe the shape of a planet moving on a Keplerian ellipse. In the absence of any other planets or forces, these elements remain fixed, as in the classic two-body problem. The sixth element, which provides the location of the planet along its orbit, can be described by one of several different measures, including the mean anomaly M , true anomaly f , eccentric anomaly E , true longitude θ , mean longitude λ , or argument of latitude v . We adopt f as our sixth element due to its intuitive geometric interpretation and with an eye towards future studies that might wish to focus on planets residing at locations close to either pericenter or apocenter.

The perturbed two-body problem has been a subject of extensive study and is applicable to several fields of astrophysics. The work of Burns (1976), subsequently popularised by Murray & Dermott (1999, pp. 54-57), provides a mechanism to obtain analytic equations for da/dt , de/dt , di/dt , and $d\Omega/dt$ arising from a small perturbative force with a given prescription for radial, tangential and normal components. This line of attack can be traced back ultimately to Gauss (see e.g., section 9.13 of Brouwer & Clemence 1961).

However, there is an alternative. Recently, a re-analysis of the derivation of Lagrange’s Planetary Equations, which describe the perturbation from a third body, revealed that a generalized gauge may be adopted in the derivation. The consequences and extensive description of this “generalized gauge theory” is provided in Efroimsky & Goldreich (2003, 2004), Gurfil (2004), Efroimsky (2005a,b, 2006), Gurfil (2007) and Gurfil & Belyanin (2008). This theory also yields analytic equations for da/dt , de/dt , di/dt , and $d\Omega/dt$ but also directly for dM/dt , arising from a perturbative force with a given prescription for each Cartesian component. In principle, either approach can be used for the

purposes of this paper; we use the latter to derive the equations of motion due to its generality and compactness.

To derive the equations of motion in orbital elements for *any* perturbing acceleration, we choose the following form, similar to Eq. (22) of Efroimsky (2005a) and Eq. (16) of Gurfil (2007):

$$\frac{d\boldsymbol{\beta}}{dt} = \mathcal{M}_1 \left[\mathcal{M}_2 \left(\Delta \mathbf{A} - \frac{d\boldsymbol{\Phi}}{dt} \right) - \mathcal{M}_3 \boldsymbol{\Phi} \right] \quad (4)$$

where $\boldsymbol{\beta} = \{a, e, i, \Omega, \omega, M_0\}$, the subscript “0” refers to the initial value, and $\boldsymbol{\Phi}$ is the gauge.

The \mathcal{M} represent matrices that are expressed entirely in terms of orbital elements, and $\Delta \mathbf{A}$ is the acceleration caused by a perturbative force on the system. Although $\Delta \mathbf{A}$ is typically written and referred to as a force, the quantity actually represents an acceleration. Equation (4) is useful because all three matrices are system-independent, and can be precomputed before any perturbative force or gauge is applied.

Assume \mathbf{A} is expressed as a column vector. The matrix \mathcal{M}_1 is then the transpose of the “Poisson Matrix”, which is composed of Poisson Brackets, and is the negative inverse of the “Lagrange Matrix”, which is composed of the Lagrange Brackets. This matrix reads:

$$\mathcal{M}_1 = \begin{pmatrix} 0 & 0 & 0 & 0 & 0 & \frac{2}{na} \\ 0 & 0 & 0 & 0 & -\frac{\sqrt{1-e^2}}{nea^2} & \frac{1-e^2}{nea^2} \\ 0 & 0 & 0 & -\frac{1}{na^2 \sin i \sqrt{1-e^2}} & \frac{1}{na^2 \tan i \sqrt{1-e^2}} & 0 \\ 0 & 0 & \frac{1}{na^2 \sin i \sqrt{1-e^2}} & 0 & 0 & 0 \\ 0 & \frac{\sqrt{1-e^2}}{nea^2} & -\frac{1}{na^2 \tan i \sqrt{1-e^2}} & 0 & 0 & 0 \\ -\frac{2}{na} & -\frac{1-e^2}{nea^2} & 0 & 0 & 0 & 0 \end{pmatrix}$$

where the orbital elements associated with each row starting at the top are a , e , i , Ω , ω and M_0 , respectively. Note that these matrix entries represent the coefficients in the appropriate form of Lagrange’s Planetary Equations. The matrices \mathcal{M}_2 and \mathcal{M}_3 are composed of partial derivatives of \mathbf{r} and \mathbf{v} , namely:

$$\mathcal{M}_2 = \begin{pmatrix} \frac{\partial r_x}{\partial a} & \frac{\partial r_x}{\partial e} & \frac{\partial r_x}{\partial i} & \frac{\partial r_x}{\partial \Omega} & \frac{\partial r_x}{\partial \omega} & \frac{\partial r_x}{\partial M_0} \\ \frac{\partial r_y}{\partial a} & \frac{\partial r_y}{\partial e} & \frac{\partial r_y}{\partial i} & \frac{\partial r_y}{\partial \Omega} & \frac{\partial r_y}{\partial \omega} & \frac{\partial r_y}{\partial M_0} \\ \frac{\partial r_z}{\partial a} & \frac{\partial r_z}{\partial e} & \frac{\partial r_z}{\partial i} & \frac{\partial r_z}{\partial \Omega} & \frac{\partial r_z}{\partial \omega} & \frac{\partial r_z}{\partial M_0} \end{pmatrix}$$

$$\mathcal{M}_3 = \begin{pmatrix} \frac{\partial v_x}{\partial a} & \frac{\partial v_x}{\partial e} & \frac{\partial v_x}{\partial i} & \frac{\partial v_x}{\partial \Omega} & \frac{\partial v_x}{\partial \omega} & \frac{\partial v_x}{\partial M_0} \\ \frac{\partial v_y}{\partial a} & \frac{\partial v_y}{\partial e} & \frac{\partial v_y}{\partial i} & \frac{\partial v_y}{\partial \Omega} & \frac{\partial v_y}{\partial \omega} & \frac{\partial v_y}{\partial M_0} \\ \frac{\partial v_z}{\partial a} & \frac{\partial v_z}{\partial e} & \frac{\partial v_z}{\partial i} & \frac{\partial v_z}{\partial \Omega} & \frac{\partial v_z}{\partial \omega} & \frac{\partial v_z}{\partial M_0} \end{pmatrix}$$

In order to compute these partial derivatives, we consider the relation between \mathbf{r} and \mathbf{v} in a fiducial inertial reference frame. These relations can be found in classical mechanical textbooks such as Taff (1985, pp. 35-36). A standard choice is:

$$\begin{pmatrix} r_x \\ r_y \\ r_z \end{pmatrix} = \mathcal{R} \begin{pmatrix} \frac{a(1-e^2)\cos f}{1+e\cos f} \\ \frac{a(1-e^2)\sin f}{1+e\cos f} \\ 0 \end{pmatrix}, \quad \begin{pmatrix} v_x \\ v_y \\ v_z \end{pmatrix} = \mathcal{R} \begin{pmatrix} \frac{-na\sin f}{(1-e^2)^{1/2}} \\ \frac{na(e+\cos f)}{(1-e^2)^{1/2}} \\ 0 \end{pmatrix} \quad (5)$$

where \mathcal{R} is the matrix

$$\mathcal{R} = \begin{pmatrix} \cos \Omega \cos \omega - \sin \Omega \sin \omega \cos i & -\cos \Omega \sin \omega - \sin \Omega \cos \omega \cos i & \sin \Omega \sin i \\ \sin \Omega \cos \omega + \cos \Omega \sin \omega \cos i & -\sin \Omega \sin \omega + \cos \Omega \cos \omega \cos i & -\cos \Omega \sin i \\ \sin \omega \sin i & \cos \omega \sin i & \cos i \end{pmatrix} \quad (6)$$

Our choice of fiducial reference frame sets the x -axis to be along the major axis of the ellipse, where the pericenter is in the positive direction. The matrices $\mathcal{M}_1, \mathcal{M}_2, \mathcal{M}_3$ are independent of the system being studied. Their computation does, however, contain some subtleties which are worth recording: i) the mean motion n in \mathcal{M}_3 is a function of a , ii) the true anomaly f is a function of the time t as well as M_0 , e and a , iii) by definition, M_0 is defined at $t = t_0$. Therefore, we need to compute the partial derivatives with respect to the true anomaly:

$$\frac{\partial f}{\partial M_0} = \frac{\partial f}{\partial E} \frac{\partial E}{\partial M_0} = \left(\frac{1+e\cos f}{\sqrt{1-e^2}} \right) \left(\frac{1+e\cos f}{1-e^2} \right) = \frac{(1+e\cos f)^2}{(1-e^2)^{3/2}} \quad (7)$$

where the expression for the first partial derivative is from Broucke (1970) – who also provides tables of partial derivatives, Lagrange Brackets and Poisson Brackets for the unperturbed two-body problem – and the second is from Kepler’s equation and from the relations between eccentric anomaly E and the true anomaly f ²:

$$\cos E = \frac{e + \cos f}{1 + e \cos f}, \quad \sin E = \frac{\sin f \sqrt{1-e^2}}{1 + e \cos f} \quad (8)$$

Further, we have:

$$\frac{\partial f}{\partial e} = \frac{\partial f}{\partial E} \frac{\partial E}{\partial e} = \left(\frac{1+e\cos f}{\sqrt{1-e^2}} \right) \left(\frac{a}{r} \sin E \right) = \frac{\sin f}{1-e^2} (2 + e \cos f) \quad (9)$$

and

$$\frac{\partial f}{\partial a} = \frac{\partial f}{\partial E} \frac{\partial E}{\partial a} = \left(\frac{1+e\cos f}{\sqrt{1-e^2}} \right) \left(-\frac{3n(t-t_0)}{2r} \right) = -\frac{3}{2}n(t-t_0) \frac{(1+e\cos f)^2}{a(1-e^2)^{3/2}} \quad (10)$$

² Note that Eq. (111) of Efroimsky (2005a) for $\partial M/\partial f$ contains a typo.

where the partial derivatives of E with respect to e and a are from Broucke (1970). Importantly, one cannot impose the condition $t = t_0$ until *after* \mathcal{M}_2 and \mathcal{M}_3 have been computed.

The time evolution with respect to E or f is often more desirable to investigators than the time evolution of M_0 , as is true in this study. We can convert one equation into another by taking the total time derivative of Kepler's equation evaluated at $t = t_0$, where $M = n(t - t_0) + M_0$. The result is:

$$\frac{dE}{dt} = \frac{1}{1 - e \cos E} \left[n + \frac{dM_0}{dt} + \sin E \frac{de}{dt} \right] \quad (11)$$

We note that the terms with the time derivatives of the semimajor axis vanish. Then we finally obtain:

$$\frac{df}{dt} = \frac{1}{1 - e^2} \left[(1 + e \cos f) \sqrt{1 - e^2} \frac{dE}{dt} + \sin f \frac{de}{dt} \right] \quad (12)$$

We choose $\Phi = 0$ in order to obtain a simply interpreted set of resulting orbital elements. However, there may be instances when choosing a non-zero gauge provides an insight or simplification to the problem considered.

As a check on these equations, we used them to re-derive the equations of motion for the two-body problem perturbed by mass loss in Veras et al. (2011).

3 General Equations

The equations below are well-suited for describing a planet on an arbitrarily wide and inclined orbit.

3.1 Orbital Element Equations

We apply:

$$\Delta \mathbf{A} = \begin{pmatrix} \mathcal{Y}_{xx}x + \mathcal{Y}_{xy}y + \mathcal{Y}_{uu}\dot{x} + \mathcal{Y}_{uv}\dot{y} \\ \mathcal{Y}_{yx}x + \mathcal{Y}_{yy}y + \mathcal{Y}_{vu}\dot{x} + \mathcal{Y}_{vv}\dot{y} \\ \mathcal{Y}_{zz}z + \mathcal{Y}_{wv}\dot{z} \end{pmatrix} \quad (13)$$

to the formalism in Section 2 in order to derive the equations of motion in terms of orbital elements:

$$\begin{aligned} \frac{da}{dt} = & \frac{2a\sqrt{1-e^2}}{n(1+e\cos f)} \left[\mathcal{Y}_{zz}C_1 \{ \sin^2 i \sin(f+\omega) \} \right. \\ & + (\mathcal{Y}_{xx}C_3 - \mathcal{Y}_{xy}C_4) \{ C_1 \sin \Omega \cos i + C_2 \cos \Omega \} \\ & \left. - (\mathcal{Y}_{yx}C_3 - \mathcal{Y}_{yy}C_4) \{ C_1 \cos \Omega \cos i - C_2 \sin \Omega \} \right] \end{aligned}$$

$$\begin{aligned}
& + \frac{2a}{1-e^2} \left[\mathcal{R}_{ww} \{C_1^2 \sin^2 i\} \right. \\
& + \mathcal{R}_{uu} \{C_1 \sin \Omega \cos i + C_2 \cos \Omega\}^2 + \mathcal{R}_{vv} \{C_1 \cos \Omega \cos i - C_2 \sin \Omega\}^2 \\
& \left. - (\mathcal{R}_{uv} + \mathcal{R}_{vu}) \{C_1 \sin \Omega \cos i + C_2 \cos \Omega\} \{C_1 \cos \Omega \cos i - C_2 \sin \Omega\} \right] \quad (14)
\end{aligned}$$

$$\begin{aligned}
\frac{de}{dt} &= \frac{(1-e^2)^{\frac{3}{2}}}{2n(1+e \cos f)^2} \left[\mathcal{R}_{zz} C_6 \{ \sin^2 i \sin(f+\omega) \} \right. \\
& + (\mathcal{R}_{xx} C_3 - \mathcal{R}_{xy} C_4) \{C_6 \sin \Omega \cos i + C_5 \cos \Omega\} \\
& - (\mathcal{R}_{yx} C_3 - \mathcal{R}_{yy} C_4) \{C_6 \cos \Omega \cos i - C_5 \sin \Omega\} \left. \right] \\
& + \frac{1}{2(1+e \cos f)} \left[\mathcal{R}_{ww} \{C_1 C_6 \sin^2 i\} \right. \\
& + \mathcal{R}_{uu} \{C_1 \sin \Omega \cos i + C_2 \cos \Omega\} \{C_6 \sin \Omega \cos i + C_5 \cos \Omega\} \\
& + \mathcal{R}_{vv} \{C_1 \cos \Omega \cos i - C_2 \sin \Omega\} \{C_6 \cos \Omega \cos i - C_5 \sin \Omega\} \\
& - \mathcal{R}_{uv} \{C_1 \cos \Omega \cos i - C_2 \sin \Omega\} \{C_6 \sin \Omega \cos i + C_5 \cos \Omega\} \\
& + \mathcal{R}_{vu} \{C_1 \sin \Omega \cos i + C_2 \cos \Omega\} \{-C_6 \cos \Omega \cos i + C_5 \sin \Omega\} \left. \right] \quad (15)
\end{aligned}$$

$$\begin{aligned}
\frac{di}{dt} &= \frac{(1-e^2)^{\frac{3}{2}} \sin i}{n(1+e \cos f)^2} \left[\mathcal{R}_{zz} \{ \cos i \cos(f+\omega) \sin(f+\omega) \} \right. \\
& - (\mathcal{R}_{xx} C_3 - \mathcal{R}_{xy} C_4) \{ \sin \Omega \cos(f+\omega) \} + (\mathcal{R}_{yx} C_3 - \mathcal{R}_{yy} C_4) \{ \cos \Omega \cos(f+\omega) \} \left. \right] \\
& + \frac{\cos(f+\omega) \sin i}{1+e \cos f} \left[\mathcal{R}_{ww} \{C_1 \cos i\} \right. \\
& - \mathcal{R}_{uu} \sin \Omega \{C_1 \sin \Omega \cos i + C_2 \cos \Omega\} + \mathcal{R}_{vv} \cos \Omega \{-C_1 \cos \Omega \cos i + C_2 \sin \Omega\} \\
& + \mathcal{R}_{uv} \sin \Omega \{C_1 \cos \Omega \cos i - C_2 \sin \Omega\} + \mathcal{R}_{vu} \cos \Omega \{C_1 \sin \Omega \cos i + C_2 \cos \Omega\} \left. \right] \quad (16)
\end{aligned}$$

$$\begin{aligned}
\frac{d\Omega}{dt} &= \frac{(1-e^2)^{\frac{3}{2}}}{n(1+e \cos f)^2} \left[\mathcal{R}_{zz} \{ \cos i \sin^2(f+\omega) \} \right. \\
& - (\mathcal{R}_{xx} C_3 - \mathcal{R}_{xy} C_4) \{ \sin \Omega \sin(f+\omega) \} + (\mathcal{R}_{yx} C_3 - \mathcal{R}_{yy} C_4) \{ \cos \Omega \sin(f+\omega) \} \left. \right] \\
& + \frac{\sin(f+\omega)}{1+e \cos f} \left[\mathcal{R}_{ww} \{C_1 \cos i\} \right. \\
& - \mathcal{R}_{uu} \sin \Omega \{C_1 \sin \Omega \cos i + C_2 \cos \Omega\} + \mathcal{R}_{vv} \cos \Omega \{-C_1 \cos \Omega \cos i + C_2 \sin \Omega\} \\
& + \mathcal{R}_{uv} \sin \Omega \{C_1 \cos \Omega \cos i - C_2 \sin \Omega\} + \mathcal{R}_{vu} \cos \Omega \{C_1 \sin \Omega \cos i + C_2 \cos \Omega\} \left. \right] \quad (17)
\end{aligned}$$

$$\frac{d\omega}{dt} = \frac{(1-e^2)^{\frac{3}{2}}}{2en(1+e \cos f)^2} \left[\mathcal{R}_{zz} \left\{ -2 \sin(f+\omega) \left[e \sin(f+\omega) + \frac{1}{2} C_8 \sin^2 i \right] \right\} \right]$$

$$\begin{aligned}
& - (\Upsilon_{xx}C_3 - \Upsilon_{xy}C_4) \{C_8 \sin \Omega \cos i - C_7 \cos \Omega\} \\
& + (\Upsilon_{yx}C_3 - \Upsilon_{yy}C_4) \{C_8 \cos \Omega \cos i + C_7 \sin \Omega\} \Big] \\
& + \frac{1}{2e(1+e \cos f)} \Big[C_1 \Upsilon_{ww} \{ -2e (\cos f \sin \omega + \cos \omega \sin f \cos^2 i) \\
& + \sin^2 i (\sin(2f + \omega) - 3 \sin \omega) \} \\
& + \Upsilon_{uu} \{C_1 \sin \Omega \cos i + C_2 \cos \Omega\} \{-C_8 \sin \Omega \cos i + C_7 \cos \Omega\} \\
& - \Upsilon_{vv} \{C_1 \cos \Omega \cos i - C_2 \sin \Omega\} \{C_8 \cos \Omega \cos i + C_7 \sin \Omega\} \\
& - \Upsilon_{uv} \{C_1 \cos \Omega \cos i - C_2 \sin \Omega\} \{-C_8 \sin \Omega \cos i + C_7 \cos \Omega\} \\
& + \Upsilon_{vu} \{C_1 \sin \Omega \cos i + C_2 \cos \Omega\} \{C_8 \cos \Omega \cos i + C_7 \sin \Omega\} \Big] \quad (18)
\end{aligned}$$

$$\begin{aligned}
\frac{df}{dt} &= \frac{n(1+e \cos f)^2}{(1-e^2)^{3/2}} + \frac{(1-e^2)^{\frac{3}{2}}}{2en(1+e \cos f)^2} \Big[\Upsilon_{zz} \{ \sin^2 i \sin(f + \omega) [C_8 + 2e \sin(f + \omega)] \} \\
& + (\Upsilon_{xx}C_3 - \Upsilon_{xy}C_4) \{C_9 \sin \Omega \cos i - C_7 \cos \Omega\} \\
& - (\Upsilon_{yx}C_3 - \Upsilon_{yy}C_4) \{C_9 \cos \Omega \cos i + C_7 \sin \Omega\} \Big] \\
& + \frac{1}{2e(1+e \cos f)} \Big[\Upsilon_{ww} \{C_1 C_9 \sin^2 i\} \\
& - \Upsilon_{uu} \{C_1 \sin \Omega \cos i + C_2 \cos \Omega\} \{-C_9 \sin \Omega \cos i + C_7 \cos \Omega\} \\
& + \Upsilon_{vv} \{C_1 \cos \Omega \cos i - C_2 \sin \Omega\} \{C_9 \cos \Omega \cos i + C_7 \sin \Omega\} \\
& + \Upsilon_{uv} \{C_1 \cos \Omega \cos i - C_2 \sin \Omega\} \{-C_9 \sin \Omega \cos i + C_7 \cos \Omega\} \\
& - \Upsilon_{vu} \{C_1 \sin \Omega \cos i + C_2 \cos \Omega\} \{C_9 \cos \Omega \cos i + C_7 \sin \Omega\} \Big] \quad (19)
\end{aligned}$$

$$= -\frac{d\omega}{dt} - \cos i \frac{d\Omega}{dt} + \frac{n(1+e \cos f)^2}{(1-e^2)^{3/2}} \quad (20)$$

where the quantities C_1, \dots, C_9 are given in Appendix A. All C terms are on the order of unity, and so the only variables in the square brackets not of the order of unity are the Υ values.

Note the remarkably simple form taken on by df/dt in Eq. (20), where the last term represents the two-body term. This form allows us to quickly derive some other results. The argument of latitude $v = f + \omega$ is a quantity which evolves with time according to:

$$\frac{dv}{dt} = -\cos i \frac{d\Omega}{dt} + \frac{n(1+e \cos f)^2}{(1-e^2)^{3/2}} \quad (21)$$

The evolution of the true longitude $\theta = v + \Omega$ is:

$$\frac{d\theta}{dt} = (1 - \cos i) \frac{d\Omega}{dt} + \frac{n(1+e \cos f)^2}{(1-e^2)^{3/2}} \quad (22)$$

3.2 Properties

Equations (14) - (20) are completely equivalent to Eqs. (1) - (3). However, Eqs. (14) - (20) let us deduce properties of planetary motion, which may not otherwise be apparent:

First, note that all the Υ terms are decoupled, allowing us to easily consider special-case physical situations by striking out the relevant terms. The rates of change of eccentricity, inclination, longitude of ascending node and longitude of pericenter ($|de/dt|$, $|di/dt|$, $|d\Omega/dt|$ and $|d\omega/dt|$) are all $\propto 1/n \propto a^{3/2}$ for the position-only Υ terms, whereas the rate of change of semimajor axis $|da/dt| \propto a/n \propto a^{5/2}$. Turning to velocity-based Υ terms, $|de/dt|$, $|di/dt|$, $|d\Omega/dt|$ and $|d\omega/dt|$ are all independent of a , whereas $|da/dt| \propto a$.

We can also deduce some properties of the evolution of special orbits. Planar orbits ($i = 0$) *will* remain planar, but circular orbits *will not* remain circular. Likewise, polar orbits *will not* remain polar. Further, the sign of di/dt will be different depending on whether $i = 90^\circ$ or $i = 270^\circ$.

As $|d\omega/dt| \propto 1/e$ and $|df/dt| \propto 1/e$, then for circular orbits, neither ω nor f are well-defined physically nor mathematically. Although Ω is not physically defined for planar orbits, Ω still remains well-defined mathematically, and remains an independent variable in all the evolution equations. In order to use a physically meaningful variable in the planar case, one must convert all of the equations to a different variable, such as $\varpi \equiv \Omega + \omega$.

Equation (22) allows us to assess how the planet appears to move from the point of view of a fixed observer: a planet will still appear to circulate around its parent star without ever reversing direction on the sky subject to all these external forces only if the planet is on a planar orbit. The extent of any modulation in the apparent motion, provided entirely by $d\Omega/dt$, increases as the planet's orbit becomes increasingly non-coplanar.

4 Adiabatic Limit

A planet on an orbit which is compact enough so that its period is smaller than the timescale of any external perturbations can be treated in the adiabatic approximation. This approximation has been utilized in many facets of planetary astronomy because the majority of exoplanets discovered are within hundreds of AU of their parent stars.

4.1 Orbital Element Equations

For the remainder of this paper, in order to simplify and focus our results, we assume $\Upsilon_{uu} = \Upsilon_{vv} = \Upsilon_{ww} = 0$. These terms do not play a role in many applications, such as tidal distortions of planetary orbits (Brasser et al., 2010), but were included in the general equations for completeness and future studies.

Here, we consider the “adiabatic” case, where averaging over the fast variables is justified. This corresponds to the following inequalities being satisfied:

$\Upsilon_{xx}/n^2 \ll 1$, $\Upsilon_{xy}/n^2 \ll 1$, $\Upsilon_{yx}/n^2 \ll 1$, $\Upsilon_{yy}/n^2 \ll 1$, $\Upsilon_{zz}/n^2 \ll 1$, $\Upsilon_{uv}/n \ll 1$, $\Upsilon_{vu}/n \ll 1$. We refer to this approximation as adiabatic, and this condition renders the equations of motion independent of the true anomaly f . We assume

$$\frac{dt}{df} = \frac{(1 - e^2)^{3/2}}{n(1 + e \cos f)^2}, \quad (23)$$

which is the unperturbed two-body term. We obtain the adiabatic limit by computing:

$$\frac{d\beta}{dt} \text{ adiabatic} = \frac{n}{2\pi} \int_0^{2\pi} \frac{d\beta}{dt} \text{ non-adiabatic} \frac{dt}{df} df \quad (24)$$

for a general variable β . Carrying out the averaging, we find:

$$\begin{aligned} \frac{da}{dt} &= \frac{a\sqrt{1-e^2} \cos i}{n} (\Upsilon_{yx} - \Upsilon_{xy}) \\ &\quad - \frac{a}{8e^2} \left[\left(-8 + 4e^2 + 8\sqrt{1-e^2} \right) \cos(2\Omega) \sin(2\omega) \cos i \right. \\ &\quad \left. + \left(\left(-2 + e^2 + 2\sqrt{1-e^2} \right) (3 + \cos 2i) \cos 2\omega \right. \right. \\ &\quad \left. \left. - 2e^2 \sin^2 i \right) \sin 2\Omega \right] (\Upsilon_{uv} + \Upsilon_{vu}) \end{aligned} \quad (25)$$

$$\begin{aligned} \frac{de}{dt} &= -\frac{5e\sqrt{1-e^2}}{2n} \cos \omega \sin \omega \sin^2 i \Upsilon_{zz} + \frac{5e\sqrt{1-e^2}}{16n} \left\{ \right. \\ &\quad + [4 \cos i \cos 2\omega \sin 2\Omega + \sin 2\omega (\cos 2\Omega (3 + \cos 2i) + 2 \sin^2 i)] \Upsilon_{xx} \\ &\quad - [4 \cos i \cos 2\omega \sin 2\Omega + \sin 2\omega (\cos 2\Omega (3 + \cos 2i) - 2 \sin^2 i)] \Upsilon_{yy} \\ &\quad - [4 \cos i \cos 2\omega \cos 2\Omega - 4 \cos i - \sin 2\omega \sin 2\Omega (3 + \cos 2i)] \Upsilon_{xy} \\ &\quad \left. - [4 \cos i \cos 2\omega \cos 2\Omega + 4 \cos i - \sin 2\omega \sin 2\Omega (3 + \cos 2i)] \Upsilon_{yx} \right\} \\ &\quad + \frac{1}{8e^3} \left[(1 - e^2) (2 - e^2 - 2\sqrt{1 - e^2}) \right. \\ &\quad \left. \times (4 \cos i \cos 2\Omega \sin 2\omega + (3 + \cos 2i) \cos 2\omega \sin 2\Omega) \right] (\Upsilon_{uv} + \Upsilon_{vu}) \end{aligned} \quad (26)$$

$$\begin{aligned} \frac{di}{dt} &= \frac{5e^2 \sin 2\omega \sin 2i}{8n\sqrt{1-e^2}} \Upsilon_{zz} + \frac{\sin i}{8n\sqrt{1-e^2}} \left\{ \right. \\ &\quad + [\sin 2\Omega (2 + 3e^2 + 5e^2 \cos 2\omega) - 10e^2 \cos i \sin 2\omega \sin^2 \Omega] \Upsilon_{xx} \\ &\quad - [\sin 2\Omega (2 + 3e^2 + 5e^2 \cos 2\omega) + 10e^2 \cos i \sin 2\omega \cos^2 \Omega] \Upsilon_{yy} \\ &\quad + [2 \sin^2 \Omega (2 + 3e^2 + 5e^2 \cos 2\omega) + 10e^2 \cos i \sin 2\omega \cos \Omega \sin \Omega] \Upsilon_{xy} \\ &\quad \left. - [2 \cos^2 \Omega (2 + 3e^2 + 5e^2 \cos 2\omega) - 10e^2 \cos i \sin 2\omega \cos \Omega \sin \Omega] \Upsilon_{yx} \right\} \\ &\quad + \frac{1}{8} \sin 2i \sin 2\Omega (\Upsilon_{uv} + \Upsilon_{vu}) \end{aligned} \quad (27)$$

$$\begin{aligned}
 \frac{d\Omega}{dt} = & \frac{\cos i (2 + 3e^2 - 5e^2 \cos 2\omega)}{4n\sqrt{1-e^2}} \Upsilon_{zz} + \frac{1}{4n\sqrt{1-e^2}} \left\{ \right. \\
 & + [\sin^2 \Omega \cos i (-2 - 3e^2 + 5e^2 \cos 2\omega) + 5e^2 \cos \Omega \sin \Omega \sin 2\omega] \Upsilon_{xx} \\
 & + [\cos^2 \Omega \cos i (-2 - 3e^2 + 5e^2 \cos 2\omega) - 5e^2 \cos \Omega \sin \Omega \sin 2\omega] \Upsilon_{yy} \\
 & - [\cos \Omega \sin \Omega \cos i (-2 - 3e^2 + 5e^2 \cos 2\omega) - 5e^2 \sin^2 \Omega \sin 2\omega] \Upsilon_{xy} \\
 & \left. - [\cos \Omega \sin \Omega \cos i (-2 - 3e^2 + 5e^2 \cos 2\omega) + 5e^2 \cos^2 \Omega \sin 2\omega] \Upsilon_{yx} \right\} \\
 & - \left(\frac{1}{2} \sin^2 \Omega \right) \Upsilon_{uv} + \left(\frac{1}{2} \cos^2 \Omega \right) \Upsilon_{vu} \quad (28)
 \end{aligned}$$

$$\begin{aligned}
 \frac{d\omega}{dt} = & \frac{5 \sin^2 \omega (\sin^2 i - e^2) - (1 - e^2)}{2n\sqrt{1-e^2}} \Upsilon_{zz} + \frac{1}{16n\sqrt{1-e^2}} \left\{ \right. \\
 & + (2C_{10} + C_{11} + C_{12}) \Upsilon_{xx} + (-2C_{10} - C_{11} + C_{12}) \Upsilon_{yy} \\
 & + (-2C_{10} \cot 2\Omega - C_{13} - 10e^2 \cos i \sin 2\omega) \Upsilon_{xy} \\
 & + (-2C_{10} \cot 2\Omega - C_{13} + 10e^2 \cos i \sin 2\omega) \Upsilon_{yx} \left. \right\} \\
 & + \frac{1}{16e^4} (-4C_{14} + C_{15}) (\Upsilon_{uv} + \Upsilon_{vu}) \quad (29)
 \end{aligned}$$

where the variables $C_{10} \dots C_{15}$ are given in Appendix A. When only vertical external forces are included, the equations yield the same stationary solution as in Brasser (2001). In the more general case, when the non-vertical external forces are included, the equations reduce to Eqs. (3)-(7) of Fouchard (2004) and the equations in Appendix A of Fouchard et al. (2006), given their assumptions about Υ and after converting their Delaunay elements to the orbital elements used in this work.

The Υ_{zz} , Υ_{xx} and Υ_{yy} terms in the expression for da/dt vanish. These terms are non-zero in all other orbital element equations. Therefore, a planet's semi-major axis is never secularly affected by vertical perturbations. In no case does orbit-averaging cause a velocity-dependent Υ term to vanish. However, in all cases, except for $d\Omega/dt$, both velocity dependent terms appear in the combination $(\Upsilon_{uv} + \Upsilon_{vu})$, which does vanish when there is no net shear on the two-body system.

5 Planar Adiabatic Limit

In the planar adiabatic limit, the general equations are greatly simplified. If the perturbations allow the planet to remain in its original orbital plane, then the vertical contributions vanish. The planet may have a planar orbit in two ways: in a prograde ($i = 0^\circ$) or retrograde sense ($i = 180^\circ$). As mentioned previously, because Ω is not defined physically for $i = 0^\circ$ or $i = 180^\circ$, we wish to eliminate it from the equations of motion in the planar case³. Trigonometric

³ Mathematically, in the planar case, $\Omega \neq 0^\circ$ and changes with time, as can be seen in Eq. (17).

manipulation demonstrates that in both the prograde and retrograde cases, both Ω and ω will vanish when a suitable angle is defined.

5.1 Prograde Equations

In the prograde case, we use the longitude of pericenter $\varpi = \Omega + \omega$ and $i = 0^\circ$. When the planet's orbit is sufficiently small, then we can impose the adiabatic approximation to obtain

$$\frac{da}{dt} = -\frac{a\sqrt{1-e^2}}{n} (\Upsilon_{xy} - \Upsilon_{yx}) - \frac{a(e^2 - 2 + 2\sqrt{1-e^2}) \sin 2\varpi}{2e^2} (\Upsilon_{uv} + \Upsilon_{vu}) \quad (30)$$

$$\begin{aligned} \frac{de}{dt} = & \frac{5e\sqrt{1-e^2}}{4n} [\sin 2\varpi (\Upsilon_{xx} - \Upsilon_{yy}) + (2\sin^2 \varpi) \Upsilon_{xy} - (2\cos^2 \varpi) \Upsilon_{yx}] \\ & - \frac{(1-e^2)(2-e^2-2\sqrt{1-e^2}) \sin 2\varpi}{2e^3} (\Upsilon_{uv} + \Upsilon_{vu}) \end{aligned} \quad (31)$$

$$\frac{di}{dt} = 0 \quad (32)$$

$$\begin{aligned} \frac{d\varpi}{dt} = & \frac{\sqrt{1-e^2}}{4n} [(3+5\cos 2\varpi) \Upsilon_{xx} + (3-5\cos 2\varpi) \Upsilon_{yy} + 5\sin 2\varpi (\Upsilon_{xy} + \Upsilon_{yx})] \\ & - \left[\frac{1}{4} (\Upsilon_{uv} - \Upsilon_{vu}) \right. \\ & \left. + \frac{(4+e^4-6e^2-4(1-e^2)^{3/2}) \cos 2\varpi}{4e^4} (\Upsilon_{uv} + \Upsilon_{vu}) \right] \end{aligned} \quad (33)$$

If $(\Upsilon_{uv} + \Upsilon_{vu}) \neq 0$, then the effect on the orbit may be drastic, even for orbiting “Hot Jupiters” at $a \approx 0.05$ AU. The terms which represent the coefficients of $(\Upsilon_{uv} + \Upsilon_{vu})$ for da/dt , de/dt and $d\varpi/dt$ are well-defined in the limits of $e \rightarrow 0$ and $e \rightarrow 1$. Further, the term for de/dt takes on a maximum of ≈ 0.06 at $e = \sqrt{2\sqrt{3}-3} \approx 0.68$. This term is independent of a and n and hence might dominate the eccentricity evolution.

Note too that the pericenter will be constantly perturbed by the external force regardless of any properties of the planet unless $\Upsilon_{uv} = \Upsilon_{vu} = 0$; even if $\Upsilon_{uv} = \Upsilon_{vu} \neq 0$ and $e = 0$, the last term in Eq. (33) will immediately become non-zero.

5.2 Retrograde Equations

The equations of motion for the completely retrograde case ($i = 180^\circ$) may take on a similar form if a different angle, an *obverse of pericenter*, ς , is defined to be the dog-leg angle equal to the sum of the longitude of descending node and the angle between the radius vector of the descending node and the pericenter of the orbit ($\varsigma \equiv 180^\circ - \Omega + 180^\circ + \omega = \omega - \Omega$). Defining this angle allows us to eliminate both Ω and ω , as in the previous subsection. Both nodes may

be physically important; the longstanding prevalence of the ascending node in dynamical parlance is perhaps due to the abundance of prograde orbits in the Solar System and, likely, exoplanetary systems, where prograde is defined with respect to the parent star's rotation.

Thus, for the planar retrograde case, we find

$$\frac{da}{dt} = \frac{a\sqrt{1-e^2}}{n} (\mathcal{R}_{xy} - \mathcal{R}_{yx}) + \frac{a(e^2 - 2 + 2\sqrt{1-e^2}) \sin 2\zeta}{2e^2} (\mathcal{R}_{uv} + \mathcal{R}_{vu}) \quad (34)$$

$$\begin{aligned} \frac{de}{dt} = & \frac{5e\sqrt{1-e^2}}{4n} [\sin 2\zeta (\mathcal{R}_{xx} - \mathcal{R}_{yy}) - (2 \sin^2 \zeta) \mathcal{R}_{xy} + (2 \cos^2 \zeta) \mathcal{R}_{yx}] \\ & + \frac{(1-e^2)(2-e^2-2\sqrt{1-e^2}) \sin 2\zeta}{2e^3} (\mathcal{R}_{uv} + \mathcal{R}_{vu}) \end{aligned} \quad (35)$$

$$\frac{di}{dt} = 0 \quad (36)$$

$$\begin{aligned} \frac{d\zeta}{dt} = & \frac{\sqrt{1-e^2}}{4n} [(3 + 5 \cos 2\zeta) \mathcal{R}_{xx} + (3 - 5 \cos 2\zeta) \mathcal{R}_{yy} - 5 \sin 2\zeta (\mathcal{R}_{xy} + \mathcal{R}_{yx})] \\ & + \left[\frac{1}{4} (\mathcal{R}_{uv} - \mathcal{R}_{vu}) \right. \\ & \left. + \frac{(4 + e^4 - 6e^2 - 4(1-e^2)^{3/2}) \cos 2\zeta}{4e^4} (\mathcal{R}_{uv} + \mathcal{R}_{vu}) \right] \end{aligned} \quad (37)$$

Note that there is at least one sign change in a term from the prograde case for each of the expressions for da/dt , de/dt and $d\zeta/dt$.

6 An Application: Galactic Tides

One potential application of the equations is the modelling of Galactic tides. There has been previous work on the effect of the Galactic tide on the Oort Cloud, as this tide strongly affects the orbital evolution of cloud comets (Heisler & Tremaine, 1986; Matese & Whitman, 1989). At the Sun's location in the Galaxy, the dominant component of the tide is caused by the Galactic disk and it acts in a direction perpendicular to the disk. For the planets in the Solar system, the Galactic tide is not generally important. A rough rule-of-thumb is that the precession due to tides $P_{\text{tide}} \approx P_{\text{ext}}^2/P_{\text{pl}}$, where P_{ext} is the orbital period of the host star in the Galaxy and P_{pl} is the orbital period of the planet around the star. For Jupiter, this gives $P_{\text{tide}} \approx 10^{14}$ yr, well in excess of a Hubble time. The timescale for the effects of the Galactic tide on the planets in the Solar system to manifest themselves is very long.

However, the growing consensus that exoplanets are ubiquitous throughout the Galaxy, together with the discovery of wide-orbit (≈ 1000 - 2500 AU) planets (e.g. Kuzuhara et al., 2011; Luhman et al., 2011), motivates the study of the effects of Galactic tides much more generally than has been done hitherto.

If the host star moving on a circular orbit in the Galaxy, then the equations for the effects of Galactic tides on the satellite of a are given by Heisler & Tremaine

(1986) and Brasser et al. (2010). In this picture, the frame of reference is centered on the star, orbiting with the star but not rotating. The frame is non-inertial. Assuming a completely flat Galactic rotation curve, the only non-vanishing planar terms are

$$\begin{aligned}\Upsilon_{xx} &= \Omega_G^2 \cos(2\Omega_G t) & \Upsilon_{xy} &= \Omega_G^2 \sin(2\Omega_G t) \\ \Upsilon_{yx} &= \Omega_G^2 \sin(2\Omega_G t) & \Upsilon_{yy} &= -\Omega_G^2 \cos(2\Omega_G t)\end{aligned}\quad (38)$$

where Ω_G is the circular frequency of the star with respect to the Galactic center. The only non-vanishing vertical term is $\Upsilon_{zz} = -4\pi G\rho_G$, where ρ_G is the local Galactic matter density (including both the luminous matter and any contribution from dark matter)⁴. As characteristic of the Galactocentric distances probed by microlensing – exemplified by OGLE 2007-BLG-050 (Batista et al., 2009) and OGLE-2003-BLG-235 (Bennett et al., 2006) – we take the location of the host star to be 3 kpc from the Galactic Center. We make the simple assumption that the Galactic rotation curve is flat with amplitude 220 kms⁻¹. Thus, for a Galactocentric distance R , we have $\Omega_G = 220 \text{ kms}^{-1}/R$. Further, at $R = 3 \text{ kpc}$, we set $\rho_G = 0.65 M_\odot \text{pc}^{-3}$, self-consistently generating the rotation curve (see e.g., Eq. 2.2 of Evans 1993).

At a distance of 3 kpc, wide-orbit planets may no longer be bound to their parent star. One way to quantify this boundary is to compute the Hill radius of the star, R_H . Equation (20) of Jiang & Tremaine (2010) suggests that $R_H = [Gm_*/(2\Omega_G^2)]^{1/3}$. Using $\Omega_G = 220 \text{ kms}^{-1}/R$, we find $R_H = 7.3 \times 10^4 \text{ AU}(R/\text{kpc})^{2/3}$. Therefore, for $R = 3 \text{ kpc}$, the Hill radius is at least $2 \times 10^5 \text{ AU}$, suggesting that any orbiting objects within that distance will remain bound.

We now apply these tides to the wide-orbit planet WD 0806-661B b, Sedna-like objects, and distant scattered disk objects. This last example provides a demonstration of when the adiabatic approximation breaks down, and hence when Eqs. (14)-(20) must be used instead of Eqs. (25)-(29). For every curve on every plot, we integrated the equations of motion in both orbital elements and Cartesian elements to check that the results are equivalent.

6.1 Wide-orbit planet WD 0806-661B b

Luhman et al. (2011) discovered the substellar companion to WD 0806-661B using direct imaging. This procedure yields a projected separation but no direct information about the orbital properties, including the eccentricity. Hence we assume the semimajor axis is equal to the projected separation ($a_0 = a \approx 2500 \text{ AU}$), and provide representative values for other orbital properties: $e_0 = 0.5$, $\varpi_0 = \Omega_0 = 0^\circ$. The dependence of the orbital evolution on the mass of the planet is negligible.

⁴ There is a sign error in the corresponding equation, the third Eq. 3, in Brasser et al. (2010).

Widest-Orbit Exoplanet

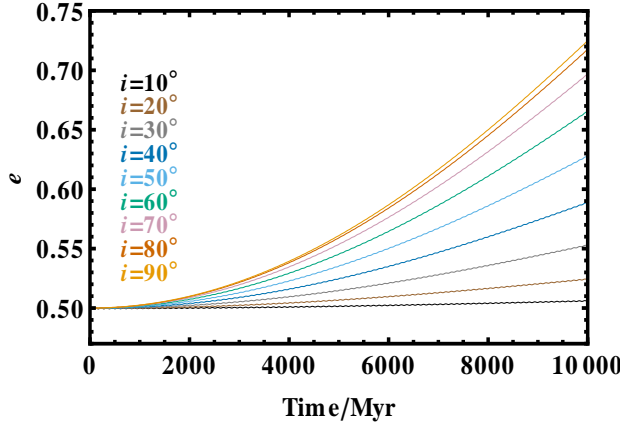


Fig. 1 The eccentricity evolution of the exoplanet with the widest-known orbit, WD 0806-661B b, due to Galactic tides. Assumed initial parameters are $a_0 = 2500$ AU, $e_0 = 0.5$, $\omega_0 = 0^\circ$, $\Omega_0 = 0^\circ$.

In Fig. 1, we plot the eccentricity evolution of WD 0806-661B b for 9 different values of i_0 over 10 Gyr, a characteristic main sequence lifetime. When $i_0 \gtrsim 42^\circ$, the eccentricity changes by over 0.1. When $i_0 \gtrsim 71^\circ$, the eccentricity changes by over 0.2. These variations illustrate that orbital signatures can significantly depend on the main sequence age of a wide-orbit planet.

6.2 Sedna-like bodies

Sedna represents the most distant member of the Solar System ever observed, and currently resides about 90 AU from the Sun (Brown et al., 2004), close to perihelion. A recent orbital fit in terms of orbital elements for Sedna has been computed by the Jet Propulsion Laboratory⁵ and shows that $a_c \approx 544$ AU, $e_c \approx 0.859$, $\omega_c \approx 310.9^\circ$ and $\Omega_c \approx 144.42^\circ$ where the subscript “c” stands for “current”. Sedna is inclined with respect to the ecliptic by about 12° . The ability for Sedna to retain unperturbed by other Solar System objects until the end of the Sun’s main sequence lifetime is uncertain; during the Sun’s post-main sequence evolution, over 6 Gyr from now, Sedna will then evolve significantly (Veras & Wyatt, 2012).

Because of this uncertainty, and because the purpose of this paper is to present the general perturbed equations of motion, we model the evolution of several Sedna-like objects. We fix $a_0 = a_c$ and $e_o = e_c$ but vary i_0 , ω_0 and Ω_0 , and run the simulations for 10 Gyr to show the full extent of the orbital change over a typical main sequence lifetime. We present our results in Fig. 2. Panels a, b and c correspond to $(\omega_0 = \omega_c, \Omega_0 = \Omega_c)$, $(\omega_0 = 225^\circ, \Omega_0 = 0^\circ)$ and

⁵ As of September 26, 2012, from <http://ssd.jpl.nasa.gov/sbdb.cgi?sstr=Sedna>

Sedna-like Bodies

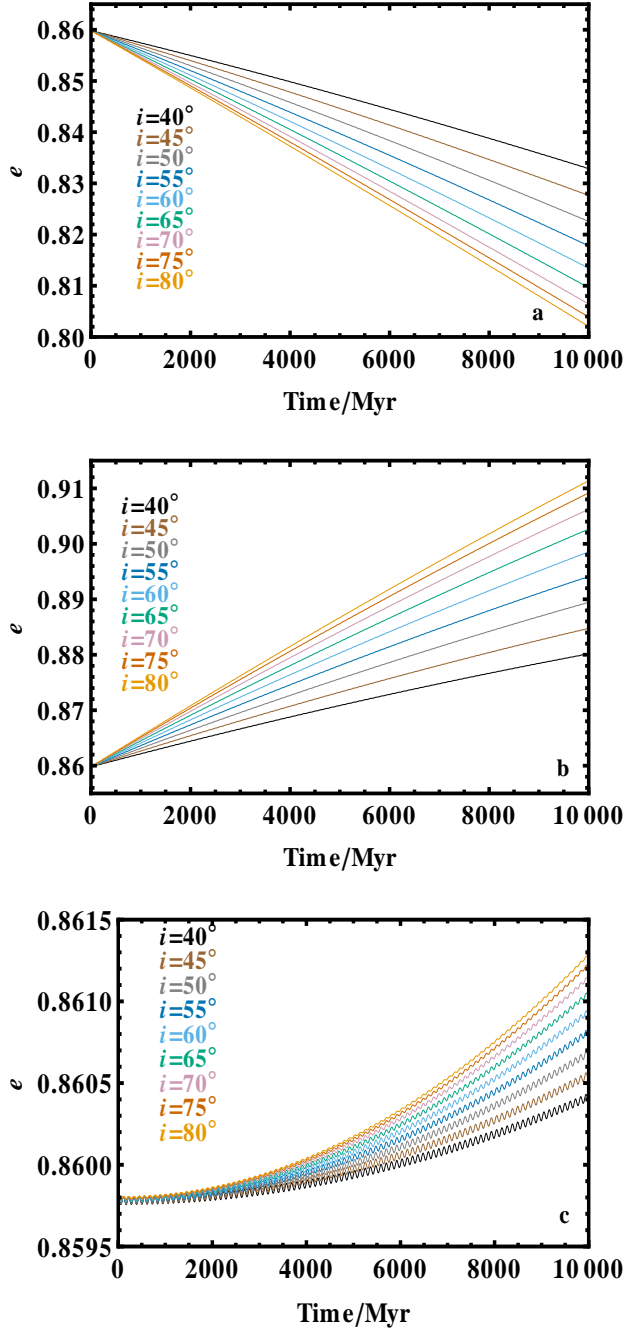


Fig. 2 The eccentricity evolution of the Sedna-like objects, all with $a_0 = 544$ AU and $e_0 = 0.859$. Panels a, b and c correspond to $(\omega_0 = \omega_c, \Omega_0 = \Omega_c)$, $(\omega_0 = 225^\circ, \Omega_0 = 0^\circ)$ and $(\omega_0 = \Omega_0 = 0^\circ)$, respectively. The modulation of the curves in panel c is due to planar tides.

Scattered Disk Bodies

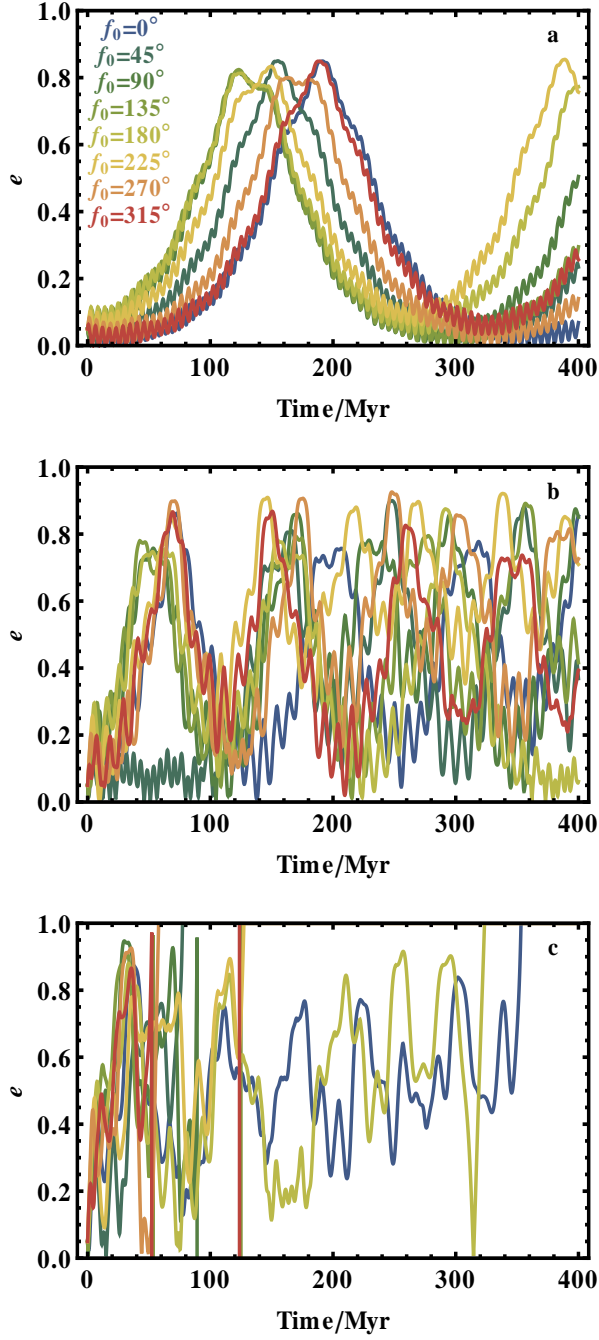


Fig. 3 The eccentricity evolution of initially nearly circular ($e_0 = 0.05$) scattered disk bodies (panel a: $a_0 = 3 \times 10^4$ AU; panel b: $a_0 = 5 \times 10^4$ AU; panel c: $a_0 = 7 \times 10^4$ AU) in systems inclined at $i = 60^\circ$ with respect to the Galactic plane. The initial true anomalies of the objects are given in the legends in the upper panel, and $\omega_0 = \Omega_0 = 0^\circ$ in all cases. In the adiabatic regime, all curves on a given plot would be equivalent. The plot demonstrates how adiabaticity is broken.

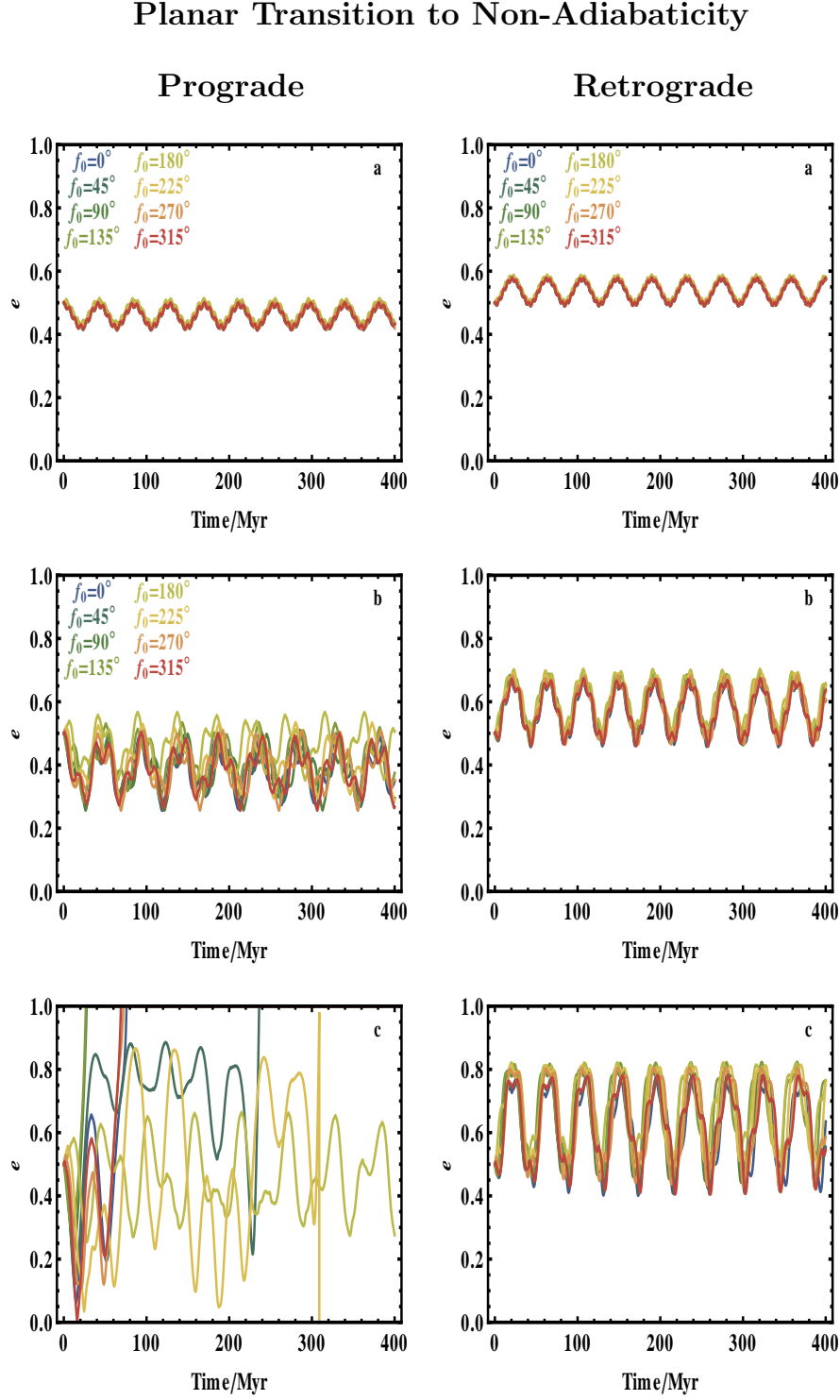


Fig. 4 A comparison of prograde planar and retrograde planar transitions to non-adiabaticity. Here, $i = 0^\circ$ so vertical tides vanish. The left panels represent the prograde case with $\varpi_0 = 0^\circ$ and the right panels represent the retrograde case with $\varsigma = 0^\circ$. The semimajor axes sampled here are equal to those in Fig. 3 (3×10^4 AU for the a panels, 5×10^4 AU for the b panels, and 7×10^4 AU for the c panels). The plot demonstrates how retrograde planets are generally more stable and more adiabatic than their prograde counterparts.

($\omega_0 = \Omega_0 = 0^\circ$), respectively. These sets of values were chosen to show different evolutionary behaviours. In panel a, the eccentricity decreases by several hundredths; in panel b, the eccentricity increases by several hundredths; in panel c, the eccentricity changes only by a few ten-thousandths. The curves in panel c also exhibit a visually discernible modulation due to the planar tides.

6.3 The breaking of adiabaticity

Here we demonstrate how adiabaticity is broken by considering outer scattered disk/inner Oort cloud-like objects with $a = 3 \times 10^4$ AU - 7×10^4 AU. We integrate the general equations (Eqs. 14-20) in Fig. 3, as well as the planar prograde and retrograde limits in Fig. 4.

Figure 3 illustrates in panel a that the transition region between adiabaticity and non-adiabaticity occurs just beyond about 3×10^4 AU. In panel b, at $a_0 = 5 \times 10^4$ AU, the sinusoidal form of the eccentricity evolution is heavily modulated, particularly after 200 Myr have elapsed. In panel c, at $a_0 = 7 \times 10^4$ AU, all of the objects have become unstable before 400 Myr have elapsed. Also note that the initially small eccentricity of the orbiting bodies do not protect them from large eccentricity variations.

Because planar tides are weaker than vertical tides, the adiabatic approximation should remain robust to larger distances in the planar case than in the non-planar case (Fig. 3). Fig. 4 demonstrates that the difference may be over a factor of 2 in semimajor axis the prograde case and over a factor of 3 in the retrograde case. Also, Fig. 4 demonstrates that retrograde objects are more stable than prograde objects. This result is intuitively sensible, given that in the planar restricted circular three-body problem, the Hill sphere is largest for a tertiary orbiting the secondary in the opposite sense of the secondary's orbit about the primary (Valtonen & Karttunen, 2006, pp. 131-133). Thus, objects on retrograde orbits are not likely to be as dynamically excited as objects on prograde orbits, or ones with nonzero inclinations.

7 Conclusions

This work provides an analytical characterization of the perturbed two-body problem. In principle, the perturbations \mathcal{T} may represent any force; the position and velocity-dependent perturbations we chose here are particularly well-suited for modelling the effect of Galactic phenomena on single-planet exosystems.

The main results are the compact form (Eq. 4), from which perturbative equations of motion may be derived analytically and quickly using an algebraic software program⁶, the general non-adiabatic non-planar equations of motion in terms of orbital elements for several types of perturbations (Eqs. 14-20), and

⁶ A *Mathematica* notebook with the necessary precomputed matrices is available from the authors.

the explicitly-expressed specific cases of these equations (Eqs. 25 - 29, Eqs. 30-33, and Eqs. 34-37). We have discussed applications to wide-separation planets as well as distant trans-Neptunian objects in our Solar system.

Further, there are numerous applications of these equations in planetary dynamics. For example, a number of studies have investigated the idea of a Galactic habitable zone (Gonzalez et al., 2001; Lineweaver et al., 2004). These are the regions in a galaxy in which a host star can harbor terrestrial planets that can support life. Others have argued that perhaps the entire Galaxy is (or has been) suitable for life, and the idea of zones is too simplistic (Prantzos, 2008). There are many processes influencing such a complex topic as habitability, including chemical, geophysical and biological factors. However, a prerequisite for life is the existence of long-lived, stable planetary orbits around a host star. In particular, the planet must remain largely unaffected by perturbations from Galactic tides, spiral arms, bars and rings, giant molecular clouds and dark matter substructures. The host star may lie on a nearly circular orbit within the Galactic disk – much like the Sun – or it may lie on a more eccentric orbit belonging to the Galactic disk, spheroid or bulge. A substantial task for dynamicists is to map out the regions of our Galaxy in which host stars can provide planetary orbits that are stable against a rich variety of perturbations. The formalism that we have developed in this paper can play an important role in this ambitious quest.

Acknowledgments

We thank the referees for useful input which has improved the quality of this paper.

References

- Anderson, D. R., Hellier, C., Gillon, M., et al. 2010. Wasp-17b: An ultra-Low density planet in a probable retrograde orbit. *ApJ*, 709, 159-167.
- Batista, V., Dong, S., Gould, A., et al. 2009. Mass measurement of a single unseen star and planetary detection efficiency for OGLE 2007-BLG-050. *A&A*, 508, 467-478.
- Bennett, D. P., Anderson, J., Bond, I. A., Udalski, A., & Gould, A. 2006. Identification of the OGLE-2003-BLG-235/MOA-2003-BLG-53 planetary host star. *ApJL*, 647, L171-L174.
- Brasser, R. 2001. Some properties of a two-body system under the influence of the Galactic tidal field. *MNRAS*, 324, 1109-1116.
- Brasser, R., Higuchi, A., & Kaib, N. 2010. Oort cloud formation at various Galactic distances. *A&A*, 516, A72 (12 pages).
- Broucke, R. A. 1970. On the matrizant of the two-Body problem. *A&A*, 6, 173-182.
- Brouwer, D., & Clemence, G. M. 1961, *Celestial Mechanics*, Academic Press, New York.

- Brown, M. E., Trujillo, C., & Rabinowitz, D. 2004. Discovery of a Candidate Inner Oort Cloud Planetoid. *ApJ*, 617, 645.
- Burns, J. A. 1976. Elementary derivation of the perturbation equations of celestial mechanics. *American Journal of Physics*, 44, 944-949
- Cox, T. J., & Loeb, A. 2008. The collision between the Milky Way and Andromeda. *MNRAS*, 386, 461-474.
- Doyle, L. R., Carter, J. A., Fabrycky, D. C., et al. 2011. Kepler-16: A transiting circumbinary planet. *Science*, 333, 1602-1606.
- Efroimsky, M., & Goldreich, P. 2003. Gauge symmetry of the N-body problem in the Hamilton-Jacobi approach. *Journal of Mathematical Physics*, 44, 5958-5977.
- Efroimsky, M., & Goldreich, P. 2004. Gauge freedom in the N-body problem of celestial mechanics. *A&A*, 415, 1187-1199.
- Efroimsky, M. 2005a. Long-Term Evolution of orbits about A precessing oblate planet: 1. The case of uniform precession. *Celestial Mechanics and Dynamical Astronomy*, 91, 75-108.
- Efroimsky, M. 2005b. Gauge freedom in orbital mechanics. *Annals of the New York Academy of Sciences*, 1065, 346-374.
- Efroimsky, M. 2006. Long-term evolution of orbits about a precessing oblate planet. 2. The case of variable precession. *Celestial Mechanics and Dynamical Astronomy*, 96, 259-288.
- Evans, N. W. 1993. Simple galaxy models with massive haloes. *MNRAS*, 260, 191
- Fouchard, M. 2004. New fast models of the Galactic tide. *MNRAS*, 349, 347-356.
- Fouchard, M., Froeschlé, C., Valsecchi, G., & Rickman, H. 2006. Long-term effects of the Galactic tide on cometary dynamics. *Celestial Mechanics and Dynamical Astronomy*, 95, 299-326.
- Gonzalez, G., Brownlee, D., & Ward, P. 2001. The Galactic habitable zone: Galactic chemical evolution. *Icarus*, 152, 185-200.
- Gurfil, P. 2004. Analysis of J2-perturbed motion using mean non-osculating orbital elements. *Celestial Mechanics and Dynamical Astronomy*, 90, 289-306.
- Gurfil, P. 2007. Generalized solutions for relative spacecraft orbits under arbitrary perturbations. *Acta Astronautica*, 60, 61-78.
- Gurfil, P., & Belyanin, S. 2008. The gauge-generalized Gylden Meshcherskii problem. *Advances in Space Research*, 42, 1313-1317.
- Heisler, J., & Tremaine, S. 1986. The influence of the galactic tidal field on the Oort comet cloud. *Icarus*, 65, 13-26.
- Jiang, Y.-F., & Tremaine, S. 2010. The evolution of wide binary stars. *MNRAS*, 401, 977-994.
- Kaib, N. A., Raymond, S. N., & Duncan, M. J. 2011. 55 Cancri: A coplanar planetary system that is likely misaligned with its star. *ApJL*, 742, L24 (6 pages).
- Kuzuhara, M., Tamura, M., Ishii, M., Kudo, T., Nishiyama, S., & Kandori, R. 2011. The widest-separation substellar companion candidate to a binary T

- Tauri star, *AJ*, 141, 119 (10 pages)
- Lineweaver, C. H., Fenner, Y., & Gibson, B. K. 2004. The Galactic habitable zone and the age distribution of complex life in the Milky Way. *Science*, 303, 59-62.
- Lissauer, J. J., Fabrycky, D. C., Ford, E. B., et al. 2011. A closely packed system of low-mass, low-density planets transiting Kepler-11. *Nature*, 470, 53-58.
- Lucas, P. W., & Roche, P. F. 2000. A population of very young brown dwarfs and free-floating planets in Orion. *MNRAS*, 314, 858-864.
- Luhman, K. L., Burgasser, A. J., & Bochanski, J. J. 2011. Discovery of a candidate for the coolest known brown dwarf. *ApJL*, 730, L9 (4 pages).
- Matese, J. J., & Whitman, P. G. 1989. The Galactic disk tidal field and the nonrandom distribution of observed Oort cloud comets. *Icarus*, 82, 389-401.
- Mayor, M., & Queloz, D. 1995. A Jupiter-mass companion to a solar-type star. *Nature*, 378, 355-359.
- Murray, C. D., & Dermott, S. F. 1999, *Solar System Dynamics*, Cambridge University Press, Cambridge.
- Prantzos, N. 2008. On the “Galactic Habitable Zone”. *Space Science Reviews*, 135, 313-322.
- Setiawan, J., Klement, R. J., Henning, T., et al. 2010. A Giant Planet Around a Metal-Poor Star of Extragalactic Origin. *Science*, 330, 1642-1644.
- Sigurdsson, S., Richer, H. B., Hansen, B. M., Stairs, I. H., & Thorsett, S. E. 2003. A young white dwarf companion to pulsar B1620-26: Evidence for early planet formation. *Science*, 301, 193-196.
- Sumi, T., et al. 2011. Unbound or distant planetary mass population detected by gravitational microlensing. *Nature*, 473, 349-352.
- Taff, L. G. 1985, *Celestial Mechanics*, Wiley-Interscience, New York.
- Triald, A. H. M. J., Collier Cameron, A., Queloz, D., et al. 2010. Spin-orbit angle measurements for six southern transiting planets. New insights into the dynamical origins of hot Jupiters. *A&A*, 524, A25 (22 pages).
- Valtonen, M., & Karttunen, H. 2006, *The Three-Body Problem*, Cambridge University Press, Cambridge.
- van der Marel, R. P., Besla, G., Cox, T. J., Sohn, S. T., & Anderson, J. 2012. The M31 velocity vector. III. Future Milky Way M31-M33 orbital evolution, merging, and fate of the Sun. *ApJ*, 753, 9 (21 pages).
- Veras, D., Wyatt, M. C., Mustill, A. J., Bonsor, A., & Eldridge, J. J. 2011. The great escape: how exoplanets and smaller bodies desert dying stars. *MNRAS*, 417, 2104-2123.
- Veras, D., & Raymond, S. N. 2012. Planet-planet scattering alone cannot explain the free-floating planet population. *MNRAS*, 421, L117-121.
- Veras, D., & Wyatt, M. C. 2012. The Solar system’s post-main sequence escape boundary. *MNRAS*, 421, 296.
- Winn, J. N., Fabrycky, D., Albrecht, S., & Johnson, J. A. 2010. Hot stars with hot Jupiters have high obliquities. *ApJL*, 718, L145-L149.
- Wolszczan, A., & Frail, D. A. 1992. A planetary system around the millisecond pulsar PSR1257 + 12. *Nature*, 355, 145-147.

Zapatero Osorio, M. R., Béjar, V. J. S., Martín, E. L., Rebolo, R., Barrado y Navascués, D., Bailer-Jones, C. A. L., & Mundt, R. 2000. Discovery of Young, Isolated Planetary Mass Objects in the σ Orionis Star Cluster. *Science*, 290, 103-107.

A Some Auxiliary Variables

Here, we collect some cumbersome variables referred to in the main body of the paper. The variables C_1, \dots, C_9 in the general case of Eqs. (14)-(20) are given by

$$\begin{aligned} C_1 &\equiv e \cos \omega + \cos (f + \omega) \\ C_2 &\equiv e \sin \omega + \sin (f + \omega) \\ C_3 &\equiv \cos i \sin \Omega \sin (f + \omega) - \cos \Omega \cos (f + \omega) \\ C_4 &\equiv \cos i \cos \Omega \sin (f + \omega) + \sin \Omega \cos (f + \omega) \\ C_5 &\equiv (3 + 4e \cos f + \cos 2f) \sin \omega + 2(e + \cos f) \cos \omega \sin f \\ C_6 &\equiv (3 + 4e \cos f + \cos 2f) \cos \omega - 2(e + \cos f) \sin \omega \sin f \\ C_7 &\equiv (3 + 2e \cos f - \cos 2f) \cos \omega + \sin \omega \sin 2f \\ C_8 &\equiv (3 - \cos 2f) \sin \omega - 2(e + \cos f) \cos \omega \sin f \\ C_9 &\equiv (3 + 2e \cos f - \cos 2f) \sin \omega - \cos \omega \sin 2f \end{aligned}$$

The variables C_{10}, \dots, C_{15} in the adiabatic limit of Eqs. (25)-(29) are given by

$$\begin{aligned} C_{10} &\equiv 5(e^2 - 2) \sin(2\omega) \sin(2\Omega) \cos i \\ C_{11} &\equiv \cos 2\Omega (1 - 6e^2 - 5(-3 + 2e^2) \cos 2\omega - 10 \cos 2i \sin^2 \omega) \\ C_{12} &\equiv 11 - 6e^2 + \cos 2\omega (5 - 10e^2) + 10 \cos 2i \sin^2 \omega \\ C_{13} &\equiv \sin 2\Omega (-1 + 6e^2 + 5(-3 + 2e^2) \cos 2\omega + 10 \cos 2i \sin^2 \omega) \\ C_{14} &\equiv \cos 2\Omega \cos i \left[e^4 + \cos 2\omega (e^4 + 4 + 2\sqrt{1 - e^2} - 2e^2 (3 + \sqrt{1 - e^2})) \right] \\ C_{15} &\equiv \cos 2\Omega \sin 2\omega (3 + \cos 2i) (e^4 + 4 + 2\sqrt{1 - e^2} - 6e^2 - 2e^2 \sqrt{1 - e^2}) \end{aligned}$$